Technical University of Denmark

Fault Monitooring and Fault Recovery Control for Position Moored Tanker

Fang, Shaoji; Blanke, Mogens

Published in:
Proceedings of Workshop on Advanced Control and Diagnosis

Publication date:
2009

Document Version
Early version, also known as pre-print

Fault Monitoring and Fault Recovery Control for Position Moored Tanker

Shaoji Fang * **Mogens Blanke** *,**

* *Centre for Ships and Ocean Structures, Norwegian University of Science and Technology, NO 7491 Trondheim, Norway, email: shaoji.fang@ntnu.no, mb@elektro.dtu.dk*
** *Automation and Control, Department of Electrical Engineering, Technical University of Denmark, DK 2800 Kgs Lyngby, Denmark*

Abstract: This paper addresses fault tolerant control for position mooring of a shuttle tanker operating in the North Sea. A complete framework for fault diagnosis is presented but the loss of a sub-sea mooring line buoyancy element is given particular attention, since this fault could lead to line breakage and risky abortion of an oil-loading operation. With significant drift forces from waves, non-Gaussian elements dominate in residuals and fault diagnosis need be designed using dedicated change detection for the type of distribution encountered. In addition to dedicated diagnosis, an optimal position algorithm is proposed to accommodate buoyancy element failure and keep the mooring system in a safe state. Detection properties and fault-tolerant control are demonstrated by high fidelity simulations.

Keywords: Fault Diagnosis, Fault-tolerant Control, Position Mooring, Change Detection, Optimal Position Control.

1. INTRODUCTION

With oil and gas exploration going into deeper waters and harsher environments, position mooring systems (PM) encounter more challenges with respect to mechanical reliability, automatic control and derived safety aspects. For thruster assisted position mooring, the main objective is to maintain the vessel's position within a limited region and keep the vessel at the desired heading such that the external environmental load is minimised. In extreme weather, the main objective changes to ensure that mooring lines avoid breakage. Related literature include Strand et al. (1998), Aamo and Fossen (2001), Nguyen and Sørensen (2007), Berntsen et al. (2008).

Safety of dynamic positioning is a prime concern in the marine industry and regulations are enforced to prevent faults in equipment to cause accidents with the system (DNV (2008)). In position mooring, accident limit status must be analysed in case of line breakage or loss of one or more mooring line buoyancy elements. Such analysis is based on the reliability of mechanical structures, and studies of the sensitivity to extreme values and associated risk for fatigue damage or line breakage with the loads from environment (Gao and Moan (2007)). Recently, automatic control for safety has received increased attention in marine research. Berntsen et al. (2006) proposed an nonlinear controller based on a structure reliability index to prevent the mooring line from getting into a low reliability zone. This algorithm mainly considered the safety status. Nguyen and Sørensen (2009) treated a switch controller for thruster-assisted position mooring. This algorithm detected the change of varying environment characteristics and switched the controller to prevent the mooring line breakage. Systematic fault tolerant control was studied for the station keeping of a marine vessel by Blanke (2005) and a structure-graph approach for fault diagnosis and control reconfiguration was validated by sea tests. Nguyen and Sørensen (2007) extended this study to the position mooring case and suggested an off-line fault accommodation design based on switching between different predetermined controllers. Mooring line buoyancy elements were not considered in these studies.

The purpose of this paper is to widen fault tolerant control design for position mooring systems to include loss of mooring line buoyancy elements. Investigating control system topology by structure-graph analysis, diagnosis system design is extended to include buoyancy elements on mooring lines. Residuals are demonstrated to be non-Gaussian, due to the nature of drift forces from waves, and a dedicated change detection and hypothesis test is designed for the particular distributions. Fault accommodation is suggested to be done by a novel algorithm that is shown optimal in avoiding mooring line breakage. The safety status of a mooring line is evaluated against the critical value of mooring line tension for the fault-accommodating control and it is illustrated, by simulations, how the optimal position algorithm is activated and prevents mooring line tension from exceeding the critical value after the loss of a buoyancy element.

The remainder of this paper is organised as follows. Section 2 addresses modeling of the position moored vessel. Section 3 presents fault diagnosis and change detection. The optimal position algorithm in fault accommodation is presented at section 4. The proposed algorithm is validated by simulations in Section 5 and conclusions are drawn in section 6.

2. SYSTEM MODELING

The purpose of the modeling is to obtain information to design fault detection and isolation (FDI) modules for essential faults and to give the prerequisites for the control reconfiguration design when faults occur. Table 1 shows the list of symbols and the block diagram in Fig. 1 illustrates the topology of function blocks in a position mooring system.

Table 1. List of symbols

symbol	Explanation
h_1, h_2, h_3	yaw measurements
$\psi, \dot{\psi}$	yaw angle and yaw rate
$\mathbf{p}_{G1}, \mathbf{p}_{G2}, \mathbf{p}_{H1}$	position measurements on Earth-fixed frame
$\mathbf{p}, \dot{\mathbf{p}}$	vessel position and velocity on Earth-fixed frame
$\mathbf{m}_1, \mathbf{m}_2, \mathbf{m}_3$	vertical reference sensor measurements
z, ϕ, θ	vessel heave, roll and pitch
$\mathbf{w}_{m1}, \mathbf{w}_{m2}, \mathbf{c}_m$	wind sensor and current measurement
$\mathbf{v}_w, \mathbf{v}_c$	wind and current velocity
$\mathbf{T}_{mbi}, \mathbf{T}_{moi}$	mooring line tension and MLBE force
$\mathbf{T}_{momi}$	mooring line tension measurement
$\mathbf{v}_m, \mathbf{v}$	vessel velocity measurement and vessel velocity in body frame
u_1, u_2, u_3	thruster input
T_1, T_2, T_3	thruster force

The basic configuration is shown in Fig. 1. There are redundant thrusters, three position measurement systems (two GPS and one hydro-acoustic position unit (HPS)), two wind sensors, three gyro compasses and three vertical reference sensors (VRS). The relative velocity through water is measured by the ship's log and mooring line tensions by tension measurement equipment (TME).

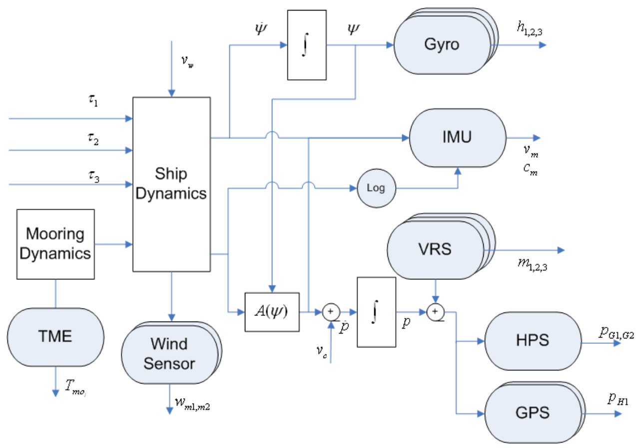

Fig. 1. Ship Configuration

In structural analysis, the model of system is considered as a set of constraints $\mathbf{C} = \{a_1, \dots, a_i, c_1, \dots c_i, d_1, \dots, d_i, m_1, \dots, m_i\}$ that are applied to a set of variables $\mathbf{X} = X \cup K$. X denotes the set of unknown variables, $K = K_i \cup K_m$ known variables: measurements (K_m), control input (K_i) etc. Variables are constrained by the physical laws applied to a particular unit. a_i denotes the constraint of thruster input, c_i denotes the algebraic constraint, d_i denotes the differential constraint, m_i are the measurements. With 3 thrusters and n mooring lines, the constrains and variables for the PM are:

$$
\begin{aligned}
a_{1..3}: \quad T_{1,2,3} &= g_t(u_1), g_l(u_2), g_l(u_2) \\
c_1: \quad \mathbf{M}\dot{\mathbf{v}} &= \mathbf{H}_{xy}\mathbf{T}[T_1, T_2, T_3]^\top + [g_w^x(v_w) \quad g_w^y(v_w)]^\top \\
&\quad + \sum_{j=1}^{n} \mathbf{A}_{mo}^{xy}(\mathbf{p}, \psi)\mathbf{T}_{moi}^{xy}(\mathbf{T}_{moi}) - \mathbf{D}[\mathbf{v} \quad \dot{\psi}]^\top \\
c_2: \quad I\ddot{\psi} &= \mathbf{H}_{\psi}\mathbf{T}[T_1, T_2, T_3]^\top + g_w^{\psi}(v_w) \\
&\quad + \sum_{j=1}^{n} \mathbf{A}_{mo}^{\psi}(\mathbf{p}, \psi)\mathbf{T}_{moi}^{\psi}(\mathbf{T}_{moi}) \\
c_3: \quad \dot{\mathbf{p}} &= A_{ve}(\psi)\mathbf{v} + \mathbf{v}_c \\
c_4: \quad \mathbf{p}_{G1} &= \mathbf{p} + \mathbf{R}(\phi, \theta, \psi)\mathbf{l}_{G1} \\
c_5: \quad \mathbf{p}_{G2} &= \mathbf{p} + \mathbf{R}(\phi, \theta, \psi)\mathbf{l}_{G2} \\
c_6: \quad \mathbf{p}_{H1} &= \mathbf{p} + \mathbf{R}(\phi, \theta, \psi)\mathbf{l}_{H1} \\
c_{2i+5}: \quad \mathbf{T}_{moi} &= g_{mo}(\mathbf{p}, \psi, \mathbf{T}_{mbi}) \\
c_{2i+6}: \quad \mathbf{T}_{mbi} &= g_{mb}(\mathbf{p}, \psi) \\
d_1: \quad \dot{\mathbf{v}} &= \frac{\partial}{\partial t}\mathbf{v} \\
d_2: \quad \dot{\mathbf{p}} &= \frac{\partial}{\partial t}\mathbf{p} \\
d_3: \quad \dot{\psi} &= \frac{\partial}{\partial t}\psi \\
d_4: \quad \ddot{\psi} &= \frac{\partial}{\partial t}\dot{\psi} \\
m_1..m_3: \quad h_{1..3} &= \psi \\
m_4: \quad \mathbf{p}_{mG1} &= \mathbf{p}_{G1} \\
m_5: \quad \mathbf{p}_{mG2} &= \mathbf{p}_{G2} \\
m_6: \quad \mathbf{p}_{mH1} &= \mathbf{p}_{H1} \\
m_7..m_9: \quad \mathbf{m}_{1..3} &= [z \quad \phi \quad \theta] \\
m_{10}: \quad \mathbf{v}_m &= \mathbf{v} \\
m_{11,12}: \mathbf{w}_{m1,m2} &= \mathbf{v}_w \\
m_{13}: \quad \mathbf{c}_m &= \mathbf{v}_c \\
m_{13+i}: \quad \mathbf{T}_{momi} &= \mathbf{T}_{moi},
\end{aligned}
$$

where $\mathbf{M}$ is mass matrix including added mass, $\mathbf{D}$ is damping matrix, I is inertia moment for yaw, $\mathbf{T}$ is thruster configuration matrix, $\mathbf{H}_{xy}$ is projection matrix for surge and sway, $\mathbf{H}_{\psi}$ is that for yaw, $\mathbf{A}_{mo}^{xy}, \mathbf{A}_{mo}^{\psi}$ is transformation matrix for horizontal mooring line tension from the Earth-fixed frame to the body frame, $\mathbf{A}_{ve}(\psi)$ is a transformation matrix for vessel velocity from Earth-fixed to body frame, $\mathbf{R}(\phi, \theta, \psi)$ is transformation matrix from the location of position reference system to the vessel coordinate origin, and $g_w^x(v_w), g_w^y(v_w), g_w^{\psi}(v_w)$ are wind force in surge, sway and yaw directions. Then according to the sets of unknown variables, input variables and measurement variables, the variables on the above constraints can be separated:

$$
\begin{aligned}
X &= \{T_1, T_2, T_3, \mathbf{T}_{mbi}, \mathbf{T}_{moi}, \mathbf{p}_{G1}, \mathbf{p}_{G2}, \mathbf{p}_{H1}, \mathbf{v}, \dot{\mathbf{v}}, \psi, \dot{\psi}, \ddot{\psi}, \\
&\quad \mathbf{p}, \dot{\mathbf{p}}, \theta, \phi, \mathbf{v}_c, \mathbf{v}_w\} \\
K_i &= \{u_1, u_2, \dots, u_k\} \\
K_m &= \{h_1, h_2, h_3, \mathbf{p}_{mG1}, \mathbf{p}_{mG2}, \mathbf{p}_{mH1}, \mathbf{m}_1, \mathbf{m}_2, \mathbf{m}_3, \mathbf{v}_m, \\
&\quad \mathbf{w}_{m1}, \mathbf{w}_{m2}, \mathbf{c}_m, \mathbf{T}_{momi}\}.
\end{aligned}
$$

3. FAULT DIAGNOSIS AND CHANGE DETECTION

3.1 Analysis of Structure

The structure graph approach is usually employed to obtain the system analytical redundancy relations for FDI. With this technique, the functional relations with measured and control variables need not be explicitly stated. SaTool is a software developed for this technique and a structure graph can be created based on implicit nonlinear constraints (Blanke (2005)).

The structural analysis finds the over-determined subsystem and a set of $10 + i$ parity relations where i is the number of mooring lines. These parity relations can be used as residual generators for fault detection in general in the system.

A deviation from normal of a constraint, i.e. a fault, will affect a parity relation if this parity relation is constructed using the constraint. Considering mooring line faults, the result is $2 + i$ such relations:

$$\begin{aligned}
r_1 =\, & c_1(a_1(u_1), a_2(u_2), c_6(m_3(h_3), m_9(\mathbf{m}_3), m_6(\mathbf{p}_{mH1})),\\
& m_3(h_3), c_{2i+5}(c_6(m_3(h_3), m_9(\mathbf{m}_3), m_6(\mathbf{p}_{mH1})),\\
& m_3(h_3), c_{2i+6}(c_6(m_3(h_3), m_9(\mathbf{m}_3), m_6(\mathbf{p}_{mH1})),\\
& m_3(h_3))), m_{12}(\mathbf{w}_{m2}), m_{10}(\mathbf{v}_m), d_3(m_3(h_3)))\\
r_2 =\, & c_2(a_3(u_3), c_6(m_3(h_3), m_9(\mathbf{m}_3), m_6(\mathbf{p}_{mH1})), m_3(h_3),\\
& c_{2i+5}(c_6(m_3(h_3), m_9(\mathbf{m}_3), m_6(\mathbf{p}_{mH1})), m_3(h_3),\\
& c_{2i+6}(c_6(m_3(h_3), m_9(\mathbf{m}_3), m_6(\mathbf{p}_{mH1})), m_3(h_3))),\\
& m_{12}(\mathbf{w}_{m2}), m_{10}(\mathbf{v}_m), d_3(m_3(h_3)),\\
& d_4(d_3(m_3(h_3))))\\
r_{5+i} =\, & m_{13+i}(\mathbf{T}_{momi}, c_{2i+5}(c_6(m_3(h_3), m_9(\mathbf{m}_3),\\
& m_6(\mathbf{p}_{mH1})), m_3(h_3), c_{2i+6}(c_6(m_3(h_3), m_9(\mathbf{m}_3),\\
& m_6(\mathbf{p}_{mH1})), m_3(h_3)))).
\end{aligned}$$

If a fault affects the residual vector, the fault is said to be is detectable. If a fault affects the unique pattern of the residual vector's elements, it is said to be structurally isolable. In the presence of only one fault, isolable constraints are $(d_2, m_1, m_2, m_3, m_7, m_8, m_9, m_{10}, m_{11}, m_{12}, m_{13+i})$. The rest are detectable.

Considering the fault on the mooring line, the dependency matrix is shown in Table 2. Violations of constraints c_{2i+5} and c_{2i+6} are only detectable but their residual vectors are unique from those of the other cases. This shows that the fault on the buoy is demonstrated from the fault of the mooring line itself. The constrains m_{13+i} are isolable and thus the fault on the tension measurement equipment can be distinguished from the fault on the mooring line, if only a single fault is present.

Table 2. Dependency Matrix

	c_{2i+5}	c_{2i+6}	m_{13+i}
r_1	1	1	0
r_2	1	1	0
r_{5+i}	1	1	1

3.2 Change Detection

After design of residual generators, hypothesis testing needs to be designed to detect the change of the residual. For the violation of constraint c_{2i+5}, c_{2i+6}, the changes happens on the residuals r_1, r_2 and r_{5+i}.

The intention of the mooring line buoyancy element (MLBE) is to reduce the static force and dynamic motion of mooring system (Mavrakos et al. (1996)). Buoyancy elements need be designed suitably, otherwise adverse effects could occur. The loss of a buoyancy element would cause deviation of static forces on the mooring line and a similar effect would occur in case of line breakage. This deviation is reflected on the residuals r_{5+i} while the acceleration deviation of PM is reflected on the residuals r_1 and r_2. All of these residuals are non-Gaussian distributed due to nonlinear vessel dynamics and nature of wave drift forces. First order wave forces will generally give Gaussian distributions and the slowly varying drift forces will give Rayleigh distribution in the residuals. Which of the two dominate will depend on the degree of natural filtering in the system dynamics. The distribution of residual r_1 is shown in Fig. 2 that can best be approximated as Rayleigh.

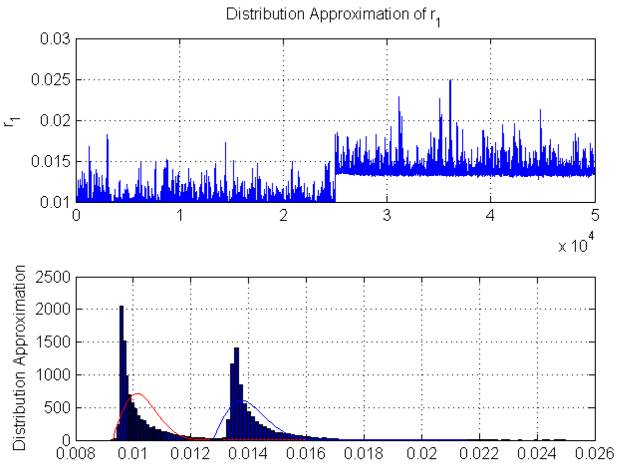

Fig. 2. Distribution Approximation of r_1

From Fig. 2, the mean value of r_1 is changed, which is described by a shifted Rayleigh density function:

$$\begin{aligned}
p(z(k)) = & \frac{(4-\pi)(z(k) - \mu_R + \frac{\sqrt{\sigma_R^2 \pi}}{\sqrt{4-\pi}})}{2\sigma_R^2}\\
& \exp[-\frac{(\sqrt{4-\pi}(z(k)-\mu_R) + \sqrt{\sigma_R^2 \pi})^2}{4\sigma_R^2}]\\
& for \quad z(k) \geq \mu_R - \frac{\sqrt{\sigma_R^2 \pi}}{\sqrt{4-\pi}},
\end{aligned}$$

where σ_R^2 is the variance of the Rayleigh distributed signal and μ_R is its mean value.

Detection of a change is suitably done using a Rao-test (Kay (1998)), which is the suitable detector for mean value change in Non-Gaussian noise while $w(k)$ is Rayleigh. The hypothesis for this case is therefore given by:

$$H_0 : z(k) = \mu_0 + w(k) \qquad k = 0, 1, \ldots, N-1$$
$$H_1 : z(k) = \mu_1 + w(k) \qquad k = 0, 1, \ldots, N-1.$$

Then the test statistics for Rao-Test is given as:

$$T_R(z) = \frac{(\frac{\partial In(p(z:\mu_R))}{\partial \mu_R}|_{\mu_R=\hat{\mu}})^2}{I(\hat{\mu})} > \gamma, \tag{1}$$

where $\hat{\mu}$ is an estimate of the signal mean value, $I(\hat{\mu})$ is the Fisher information. Then the partial derivative of the probability density function is found as:

$$\frac{\partial In(p(z,\mu_R))}{\partial \mu_R} = \frac{4-\pi}{2\sigma_R^2}\sum_{n=0}^{N-1}(z(k) - \mu_R + \sqrt{\frac{\pi\sigma_R^2}{4-\pi}}) - \frac{2\sigma_R^2}{4-\pi}\sum_{n=0}^{N-1}\frac{1}{z(k) - \mu_R + \sqrt{\frac{\pi\sigma_R^2}{4-\pi}}}. \tag{2}$$

The Fisher information with the Rayleigh distribution is found to be:

$$I(\mu_R) = \frac{N(4-\pi)}{2\sigma_R^2}\sqrt{\frac{\pi\sigma_R^2}{4-\pi}} + \frac{2\sigma_R^2}{(4-\pi)^2} \sum_{n=0}^{N-1}\frac{1}{(\sqrt{4-\pi}(z(k)-\mu_R) + \sqrt{\pi\sigma_R^2})^2}, \tag{3}$$

where μ_R can be estimated online as $\mu_R = \hat{\mu}$ and σ_R is assumed to be unchanged. Then the test statistics can be deducted based on Equ. 1 with Equ. 2 and Equ. 3.

The above detector derived from Equ. 1-3 is only available for the data bigger than zero and the Rayleigh density function is shifted to have the mean value μ_R. Then the data needs to satisfy:

$$\epsilon(k) = \max(z(k) - \mu_R + \sqrt{\frac{\sigma_R^2\pi}{4-\pi}}, 0). \tag{4}$$

In order to be able to use the same threshold for all times of tests, data are normalised and the result of the test statistics is shown in Fig. 3.

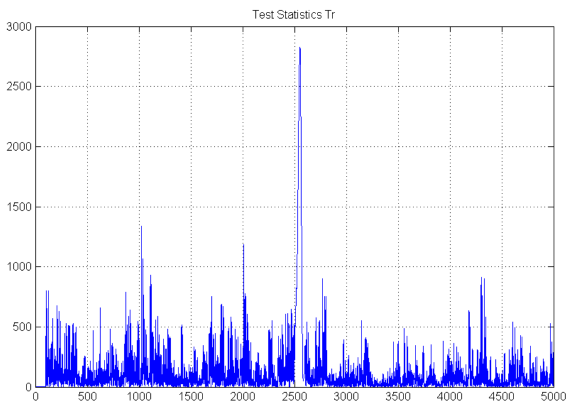

Fig. 3. Time history of test statistics

As shown in Fig. 3, test statistics is quite fluctuating in the first 2500 s while the system comes to a steady state. The loss of one buoy happens at time 2500 s and is rapidly detected.

4. FAULT TOLERANT CONTROL

4.1 Controller design

The controller objective is to maintain the vessel's position in a limited region and keep the vessel at the desired heading such that the external environmental load is minimised. Another function is to avoid the line breakage and keep the mooring system at a safe status. An optimal position algorithm is designed to meet the second objective. It is common to use multi-variable PID control in PM systems with the structure,

$$\boldsymbol{\tau}_{thr} = -\mathbf{K}_i\mathbf{R}^T(\psi)\int \hat{\boldsymbol{\eta}}_e dt - \mathbf{K}_p\mathbf{R}^T(\psi)\hat{\boldsymbol{\eta}}_e - \mathbf{K}_d\hat{\boldsymbol{\nu}}_e \tag{5}$$

where $\hat{\boldsymbol{\eta}}_e = \hat{\boldsymbol{\eta}} - \boldsymbol{\eta}_d$; $\hat{\boldsymbol{\nu}}_e = \hat{\boldsymbol{\nu}} - \boldsymbol{\nu}_d$ are the position and velocity errors; $\boldsymbol{\eta}_d$ and $\boldsymbol{\nu}_d$ the desired position and velocity vectors; $\mathbf{K}_d$, $\mathbf{K}_i$ and $\mathbf{K}_d \in \mathbb{R}^{3\times 3}$ are gain matrices. ψ is measured heading angle. However, in case of certain faults, this controller can not provide sufficiently good control.

4.2 Optimal position chasing

To maintain all the mooring lines at a safe state, an optimal position algorithm is proposed here. Position mooring is restricted to a safety region, which is normally defined from considering static mooring line tension (Nguyen and Sørensen (2007)). A reliability index was also used to evaluate this region (Berntsen et al. (2008)). This section proposes a new algorithm based on the mooring line tension for use in on-line fault-tolerant control.

First, a reference model is used for obtaining smooth transitions in the chasing of the optimal position set-point. This reference model refers to Fossen (2002) and it produces a smooth position reference that are the inputs to the position control law in Equation (5).

Optimal set-point is achieved through a quadratic object function based on every mooring line horizontal tension,

$$L(T_{m1}, T_{m2}, \ldots, T_{mn}) = \sum_{i=1}^{n}\alpha_i T_{mi}^2 \tag{6}$$

where T_{mi} is the ith horizontal mooring line tension and α_i the weighting factor. For mooring system fixed on a turret, motion of a mooring line is shown in Fig. 4. The ith mooring line is fixed on the sea floor with an anchor at point (x_i^a, y_i^a). In another side, mooring line is connected to the turret at terminal point (TP) (x_{io}, y_{io}) and centre of turret is at point (x_o, y_o). From point (x_{io}, y_{io}) to point (x_i, y_i), TP moves with distance Δr and length of the mooring is changed from h_{io} to h_i. Meantime, angle of the mooring in the Earth-fixed frame is changed from β_{io} to β_i. For the mooring system connected to a turret, TP is assumed to be connected in the turret centre and the body frame is set on the centre of the turret. Thus Δr also denotes the vessel change in position and β in direction.

Horizontal mooring line tension T_i at point (x_i, y_i) is expressed as a function of Δr and β as:

$$T_i = T_{oi} + c_i\Delta h = T_{oi} - c_i\Delta r\cos(90^\circ - \beta - \beta_{oi}) = T_{oi} - c_i\Delta r\sin(\beta + \beta_{oi}),$$

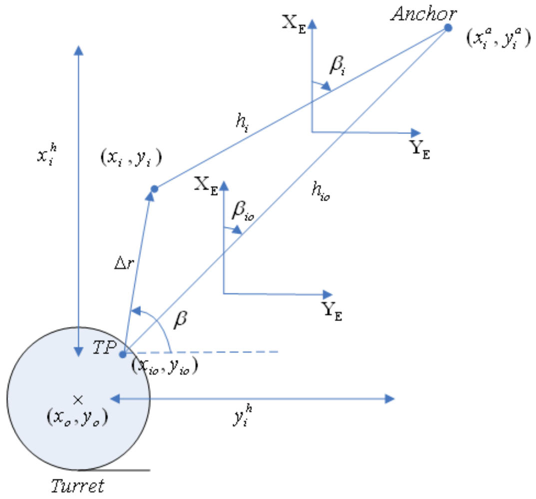

Fig. 4. Motion of one mooring line

where T_{oi} is the tension in working point (x_o, y_o), c_i is incremental stiffness tension at present instantaneous working point according to Strand et al. (1998).

The optimal position algorithm is generally used in the case that tension of each line is different. One application is that mooring line is in a risk of breakage. Then evaluation for horizontal mooring line tension could be $T_{mi} = T_{ci} - T_i$ once the ith mooring line has a risk to be beyond the critical tension T_{ci}. Or weighting coefficient w_i is adjusted to emphasise the importance of a certain mooring line. In the case of lost MLBE, this algorithm is also very useful. For notation simplification, the case of all the mooring lines at a risk is presented as:

$$L(T_{m1}, T_{m2}, \ldots, T_{mn}) = \sum_{i=1}^{n} \alpha_i (T_{ci} - T_i)^2 \qquad (7)$$

By solving the equations where the partial derivative of Equ. (7) with respect to the optimal increment of the vessel position and the optimal direction of this increment are set to zero, the minimum value of the object function is hence identified. The optimal increment of vessel position and the optimal direction of this increment is found to be:

$$\Delta r = \frac{K_{11} \sin \beta_{opt} + K_{12} \cos \beta_{opt}}{K_{21} \sin^2 \beta_{opt} + 2K_{22} \sin \beta_{opt} \cos \beta_{opt} + K_{23} \cos^2 \beta_{opt}}$$

$$\beta_{opt} = \mathrm{tg}^{-1} \frac{K_{11}K_{23} - K_{12}K_{22}}{K_{21}K_{12} - K_{11}K_{22}},$$

where:

$$\begin{aligned}
K_{11} &= \alpha_1 (T_{c1} - T_{o1}) c_1 \cos \beta_{01} + \alpha_2 (T_{c2} - T_{o2}) c_2 \cos \beta_{02} \\
&\quad + \cdots + \alpha_n (T_{cn} - T_{on}) c_n \cos \beta_{0n} \\
K_{12} &= \alpha_1 (T_{c1} - T_{o1}) c_1 \sin \beta_{01} + \alpha_2 (T_{c2} - T_{o2}) c_2 \sin \beta_{02} \\
&\quad + \cdots + \alpha_n (T_{cn} - T_{on}) c_n \sin \beta_{0n} \\
K_{21} &= \alpha_1 c_1^2 \cos^2 \beta_{01} + \alpha_2 c_2^2 \cos^2 \beta_{02} + \cdots + \alpha_n c_n^2 \cos^2 \beta_{0n} \\
K_{22} &= \alpha_1 c_1^2 \sin \beta_{01} \cos \beta_{01} + \alpha_2 c_2^2 \sin \beta_{02} \cos \beta_{02} \\
&\quad + \cdots + \alpha_n c_n^2 \sin \beta_{0n} \cos \beta_{0n} \\
K_{23} &= \alpha_1 c_1^2 \sin^2 \beta_{01} + \alpha_2 c_2^2 \sin^2 \beta_{02} + \cdots + \alpha_n c_n^2 \sin^2 \beta_{0n}.
\end{aligned}$$

Finally the updated position and heading set-point is:

$$\eta = \eta_o + \Delta r [\cos \beta_{opt} \quad \sin \beta_{opt} \quad 0]^\top . \qquad (8)$$

5. SIMULATION

The purpose of this simulation is to validate the proposed fault tolerant control strategy for the PM vessel subjected to lost MLBE. The simulation is carried out with Marine System Simulator (MSS) developed at Norwegian University of Science and Technology (NTNU).

A turret-moored floating production, storage and offloading vessel model from the MSS library is used here. The turret mooring system consists of four mooring lines with buoys shown in Fig. 5. Mooring length is $L = 2250m$, diameter is $D = 0.08m$, cable density is $\rho_c = 5500kg/m^3$, added mass coefficient $C_{mn} = 1.5$, normal drag coefficient is $C_{dn} = 1$, tangential drag coefficient is $C_{dt} = 0.3$. A buoy is connected at position $s = 750m$ along unstretched mooring line. Buoy is 8 $\times 10^4$ kg with volume $V = 120m^3$. Added mass of buoy is 5.8 $\times 10^4$ kg and drag force coefficient is $C_{dx} = 0.7$. Working water depth is 1000 m and mooring lines are simulated from finite element model with RIFLEX software(MARINTEK (2003)). Each mooring line consists of 300 elements. From touch point to the buoy, 100 elements are made and there are 200 from the buoy to the terminal point.

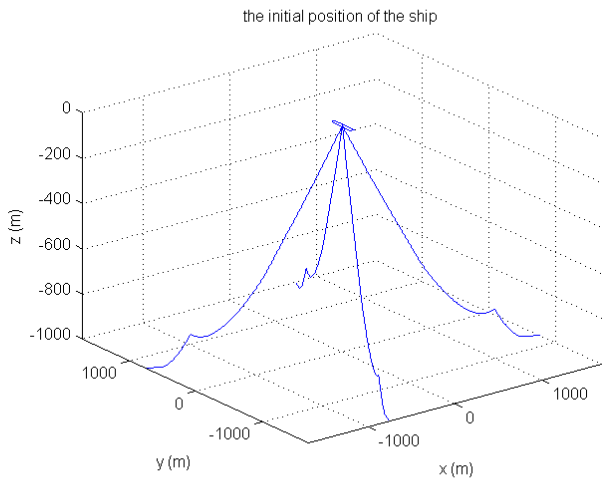

Fig. 5. Initial condition of simulation

For the external force, JONSWAP wave spectrum is used with wave height $H_s = 2m$ and wave period $T_p = 5s$. The current is $v_c = 1m/s$ at the top and decreases to 0.2 m/s at depth 500 m. At the bottom of sea floor, current is 0 m/s. Wind speed is $v_w = 8m/s$ and direction is 45 deg.

5.1 Simulation with lost MLBE

A buoy lost is an event where mooring lines could come beyond critical tension. The simulation about this effect is shown in Fig. 6-8. In the simulation, No.2 mooring line tension increases after the buoy is lost at $t = 2500$ s and then mooring system comes into new equilibrium status where No.2 mooring line is still in safe situation. The tension analysis for mooring line with MLBE must be done before employing the MLBE and thus in the structural view, the mooring line with or without buoy should be

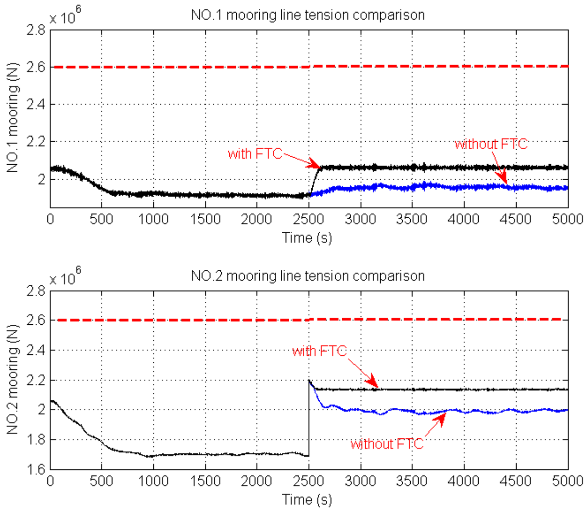

Fig. 6. No.1 and No.2 mooring line tension

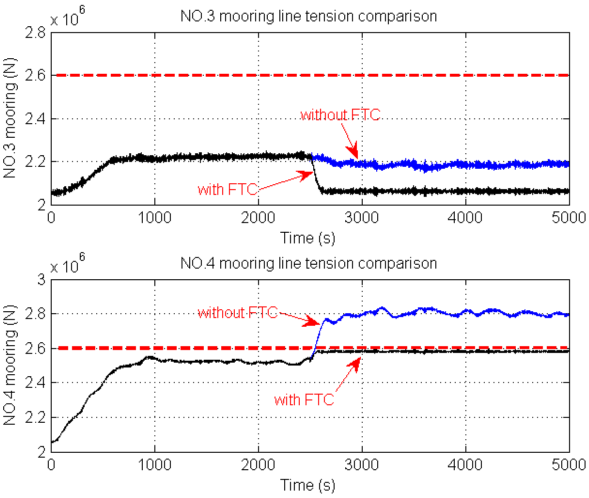

Fig. 7. No.3 and No.4 mooring line tension

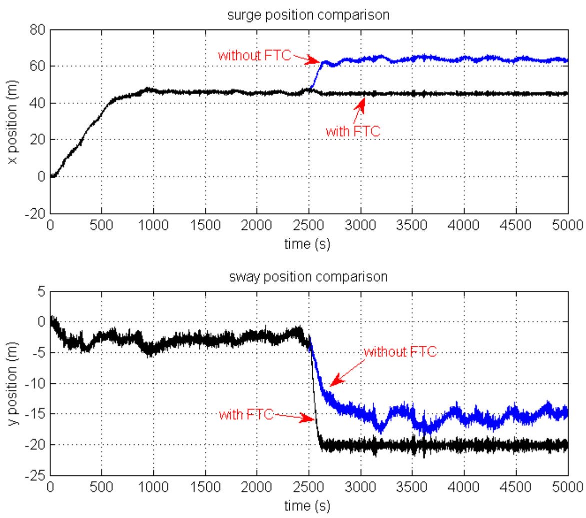

Fig. 8. Time variation of x and y positions

safe. Mooring line 4 tension increases but is kept below its critical value. Mooring lines 1 and 3 are not critical as their tensions are well below critical.

With the optimal position algorithm, PM moves to the optimal position. Mooring line 4 comes close to critical tension, but the mooring system remains safe with all lines below critical tension. The new algorithm could be extended to simultaneous faults and protect PM for more than one mooring line in danger.

6. CONCLUSION

Fault tolerant control for position mooring was analysed in this paper with specific emphasis given to the case of loss of a mooring line buoyancy element. Position mooring control was analysed with the dynamics of mooring line buoys attached and structural analysis was employed to get residuals to detect changes that could indicate faults in the system. An optimal position algorithm was suggested to avoid critical safety levels of mooring line tension. The proposed algorithm monitored the influence from external environment directly from mooring line tension, and the control algorithm was able to simultaneously control tension of more than one mooring line, even when this was close to critical levels.

REFERENCES

Aamo, O. and Fossen, T. (2001). Finite element modelling of moored vessels. *Mathematical and Computer Modelling of Dynamical Systems*, 47–75.

Berntsen, P., Aamo, O., and Leira, B. (2006). Dynamic positioning of moored vessels based on structure reliability. *Proc. 45th IEEE CDC*, 5906–5911.

Berntsen, P., Aamo, O., and Leira, B. (2008). Structural reliability-based control of moored interconnected structures. *Control Engineering Practice*, 495–504.

Blanke, M. (2005). Diagnosis and fault-tolerant control for ship station keeping. *Proc. 13th Mediterranean Conference on Control and Automation.*

DNV (2008). Positon mooring. DNV-OS-E301.

Fossen, T.I. (2002). *Marine Control System.* Marine Cybernetics, Norway.

Gao, Z. and Moan, T. (2007). Sensitivity study of extreme value and fatigue damage of line tension in mooring system with one line failure under varying annual environmental condition. *Proc. 17th ISOPE.*

Kay, S. (1998). *Fundamentals of Statistical Signal Processing, Volume 2: Detection Theory.* Prentice Hall.

MARINTEK (2003). User manual, version 3.2.3. *MARINTEK report no. 519619.*

Mavrakos, S., Papazoglou, V., Triantafyllou, M., and Hatjigeorgiou, J. (1996). Deep water mooring dynamics. *Marine Structure*, 181–209.

Nguyen, D. and Sørensen, A. (2007). Setpoint chasing for thruster-assisted position mooring. *Proc. 26th OMAE conference*, 553–560.

Nguyen, D. and Sørensen, A. (2009). Switch control for thruster-assisted position mooring. *Control Engineering Practice*, 985–994.

Strand, J., Sørensen, A., and Fossen, T. (1998). Design of automatic thruster assisted position mooring systems for ships. *Modelling, Identification and Control*, 61–75.